

5947

**SYMPOSIUM: SYNTHESIS AND SECRETION OF MILK PROTEIN AND FAT**

**Regulation of the Soluble Form of Nicotinamide Adenine  
Dinucleotide Phosphate-Specific Isocitrate Dehydrogenase  
from Lactating Bovine Mammary Gland: Effects of Metabolites  
on Activity and Structure<sup>1</sup>**

**HAROLD M. FARRELL, JR., EDWARD D. WICKHAM,  
VIRGINIA L. SEERY, and THOMAS F. KUMOSINSKI**  
Agricultural Research Service, USDA  
Eastern Regional Research Center  
600 East Mermaid Lane  
Philadelphia, PA 19118

## SYMPOSIUM: SYNTHESIS AND SECRETION OF MILK PROTEIN AND FAT

### Regulation of the Soluble Form of Nicotinamide Adenine Dinucleotide Phosphate-Specific Isocitrate Dehydrogenase from Lactating Bovine Mammary Gland: Effects of Metabolites on Activity and Structure<sup>1</sup>

HAROLD M. FARRELL, JR., EDWARD D. WICKHAM,  
VIRGINIA L. SEERY, and THOMAS F. KUMOSINSKI  
Agricultural Research Service, USDA  
Eastern Regional Research Center  
600 East Mermaid Lane  
Philadelphia, PA 19118

#### ABSTRACT

The cytosolic form of NADP<sup>+</sup>: isocitrate dehydrogenase, a primary source of the NADPH required for de novo fatty acid synthesis in lactating bovine mammary gland, was studied to determine possible mechanisms of regulation by metabolites. The enzymatic reduction of NADP<sup>+</sup> exhibits lag-burst (hysteretic) kinetics that are eliminated by the noncatalytic binding of the substrate, a complex (1:1) of a metal ion (Mn<sup>2+</sup> or Mg<sup>2+</sup>) and isocitrate. Preincubation of the enzyme with metal-citrate complex also nearly abolished the lag or activation time. In steady-state experiments, analyses of velocity versus metal-citrate complex as a binding isotherm, following the assumptions of Wyman's theory of thermodynamic linkage, showed that binding of metal-citrate complex could both stimulate and inhibit the enzyme. This analysis suggested hyperactivation by binding to sites with an average dissociation constant of .25 mM, inhibition by binding to sites with an average dissociation constant of 3.83 mM, and modulation (reactivation) by binding to sites with an average dissociation constant of 1.54 mM. Conformational changes induced by the binding of ligands were assessed using circular dichroism. The results suggest that bind-

ing of metal-isocitrate induces a conformational transition involving tyrosyl residues that is related to the altered kinetic processes. Reexamination of Michaelis-Menten kinetics using non-linear regression analysis also demonstrated hyperactivation of enzyme activity by metal-isocitrate with a dissociation constant equal to 21  $\mu$ M (which is nearly seven times greater than the Michaelis constant). Concentration ranges observed for these transitions are compatible with physiological conditions, suggesting that complexes of metal-citrate and metal-isocitrate serve to modulate the activity of NADP<sup>+</sup>: isocitrate dehydrogenase.

(Key words: enzyme regulation, lipid synthesis, milk secretion)

**Abbreviation key:** CD = circular dichroism, IDH = isocitrate dehydrogenase,  $K_d$  = dissociation constant,  $K_m$  = Michaelis constant, MC = metal-citrate, MS = metal-isocitrate,  $V_{max}$  = maximum velocity.

#### INTRODUCTION

The enzyme, NADP<sup>+</sup>-dependent isocitrate dehydrogenase (IDH) [threo-D<sub>s</sub>-isocitrate: NADP<sup>+</sup> oxidoreductase (decarboxylating) EC 1.1.1.42], can serve as source of NADPH for synthesis of metabolic end products in a variety of tissues, such as adrenal gland, kidney, and liver (7, 17). In lactating ruminant mammary gland, this enzyme may be a primary source of the NADPH required for fatty acid and cholesterol synthesis (2, 22). A survey of the distribution of Krebs cycle enzymes in bovine mammary tissue showed that NADP<sup>+</sup>: IDH is predominately cytosolic (>90%) in na-

Received September 26, 1991.

Accepted December 13, 1991.

<sup>1</sup>Mention of brand or firm names does not constitute an endorsement by the US Department of Agriculture over others of a similar nature not mentioned.

ture and that little or no NAD<sup>+</sup>:IDH activity is present (11). The latter enzyme is allosterically regulated by metabolites and is thought to be a major point of control of Krebs cycle activity (4, 16); its absence in bovine mammary gland raises the question as to what might control this important step in mammary Krebs cycle activity. Although the kinetics of NADP<sup>+</sup>:IDH from heart tissue has been investigated in detail (7, 8, 24), Plaut et al. (25) have demonstrated that the heart enzyme is of mitochondrial origin, whereas the purified mammary enzyme is clearly a cytosolic or soluble form. These two forms of the enzyme are now known to be immunologically and electrophoretically distinct (25), so investigations of the kinetic properties of the cytosolic enzyme and the effects of metabolites on its structure and activity were undertaken to gain further insight into possible mechanisms that may regulate this enzyme in lactating bovine mammary gland.

## MATERIALS AND METHODS

### Materials

All coenzymes, substrates, and biochemicals used in this study were purchased from either Sigma Chemical Co. (St. Louis, MO) or Calbiochem (San Diego, CA). [1,5-<sup>14</sup>C]Citric acid (110 mCi/mmol) was from Amersham Corp. (Arlington Heights, IL). Blue Sepharose CL-6B and Sephacryl S-200 were products of Pharmacia (Piscataway, NJ), and DE-32 was obtained from Whatman (Clifton, NJ). All other chemicals were reagent grade.

Whole mammary glands from cows of known good health and productivity were obtained through the cooperation of J. E. Keys and R. H. Miller of USDA (Beltsville, MD). The whole mammary glands were obtained at slaughter, trimmed to remove adipose tissue, and sectioned into pieces approximately 10 × 15 × 5 cm. The tissue was frozen on dry ice and stored at -80°C until used. The NADP<sup>+</sup>:IDH was isolated as described by Farrell (9).

### Enzyme Assays

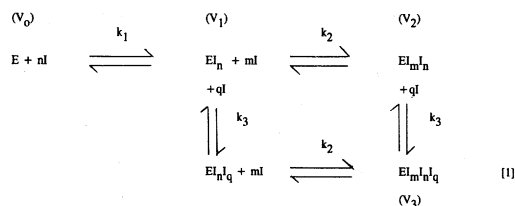
Activity of NADP<sup>+</sup>:IDH was measured at 25°C by monitoring the increase in absorbance at 340 nm. The standard reaction mixture consisted of 100 mM Tris·HCl at pH 7.4, 1.10 mM MnSO<sub>4</sub>, 1.50 mM DL-isocitrate, and 110 μM NADP<sup>+</sup> in a total volume of 2.70 ml; 10 to 50

μl of enzyme were added to start the reaction. Throughout this study, only Mn<sup>2+</sup> was used; therefore, "metal" will be used to refer to Mn<sup>2+</sup>, although Mg<sup>2+</sup> can replace it with only minor effects (9). Concentrations of metal-citrate (MC), metal-isocitrate (MS), and free metal ion were computed as previously described (33). One enzyme unit catalyzes the formation of 1.0 μmol/min of NADPH at 25°C. Specific activity is defined as enzyme units per milligram of protein. Stopped flow experiments were carried out and monitored at 340 nm on a Durrum stopped flow spectrophotometer (Dionex, Sunnyvale, CA), equipped with a storage oscilloscope as previously described (8).

### Data Analysis Steady-State Kinetics

Nonlinear regression analyses of progress curves and variance of other parameters with concentration were carried out using the program Abacus, which is based on the Gauss-Newton iterative method and which was developed by William Damert, Eastern Regional Research Center. Choices between fits of models and statistical methods of analysis of the nonlinear fits were as described by Meites (21). Change in the observed velocity of an enzyme by substrate or an inhibitor are most likely thermodynamically linked to binding (12, 34) to the enzyme.

Thus, (Figure 3a) for an enzyme (E), of which the velocity (V) is affected by an inhibitor (I) in various ways, the following equilibria were assumed to exist in the steady-state experiments for the already activated enzyme:



Preliminary analyses of Figure 3a indicated three responses of velocity to MC. The simplest mathematical description of this observation yielding the best fit to the data is

$$\begin{aligned}
 V_{\text{obs}} = & V_0 f_E + V_1 (f_{E_i} - f_{E_i I_m} - f_{E_i I_m I_q}) \\
 & + V_2 f_{E_i I_m} + V_3 f_{E_i I_m I_q} \quad (2)
 \end{aligned}$$

where  $V_0$  is the apparent maximum velocity ( $V_{\max}$ ) in the absence of concentration-dependent binding of an effector molecule (I), and  $V_1$  through  $V_3$  represent velocities contributed by each state represented in the stoichiometric Equation [1] as modulated by the fraction (f) of enzyme in each state. The analysis presupposes that  $k_1 > k_2 \sim k_3$  and that  $k_1$ ,  $k_2$ , and  $k_3$  represent binding to noninteracting classes of independent sites. Other models were tested, including three cooperative sites, one independent site, and two cooperative sites, but the fits were poor and not justified statistically (21). Following the method of Wyman, thermodynamic linkage of the binding of inhibitor to change in velocity can be derived by substituting terms for binding of inhibitor into Equation [2] as previously described (10). For data following the behavior shown in Figure 3a, the equations are

$$\begin{aligned}
 V_{\text{obs}} = & \frac{V_0}{1 + k_1^n I^n} \\
 & + V_1 \left[ \frac{k_1^n I^n}{1 + k_1^n I^n} - \frac{k_2^m I^m}{(1 + k_2^m I^m)(1 + k_3^q I^q)} \right. \\
 & \left. - \frac{k_2^m I^m k_3^q I^q}{(1 + k_2^m I^m)(1 + k_3^q I^q)} \right] \\
 & + \frac{V_2 k_2^m I^m}{(1 + k_2^m I^m)(1 + k_3^q I^q)} \\
 & + \frac{V_3 k_2^m I^m k_3^q I^q}{(1 + k_2^m I^m)(1 + k_3^q I^q)} \quad [3]
 \end{aligned}$$

The association constants ( $k_i$ ) and the terms  $n$ ,  $m$ , and  $q$  have the meanings expressed in the stoichiometric Equation [1]. Because Michaelis-Menten conditions are employed, the inhibition concentration is taken to be the total concentration of MC complex fixed at the beginning of the experiment. The data were fitted by nonlinear regression analysis using integer values for  $n$ ,  $m$ , and  $q$ ; Equation [3] implies no interaction among the three classes of sites. In each case, the iterative analysis was carried out until a minimum value for the root mean square was found. The data were tested by  $F$  test for improved fit at each change in the integer values (21).

#### Binding Studies

The binding of [ $^{14}\text{C}$ ]MC to IDH was studied at 25°C using Millipore Ultrafree PF-filter

units (Millipore, Bedford, MA) containing polysulfone membranes with a nominal cutoff of 30,000 molecular weight for proteins. The initial total concentrations of MC were determined as just described.

Enzyme (40  $\mu\text{M}$ ) and MC (stock concentration, 81.3 mM citrate with a specific activity of 53.3 cpm/nmol) were allowed to equilibrate at 25°C in .1  $M$  Tris-HCl, pH 7.4, for 10 min. The samples (300  $\mu\text{l}$ ) were filtered to near dryness under  $\text{N}_2$  at 25 psi; 100  $\mu\text{l}$  of Tris-HCl were then filtered to purge the Luer tip of the cartridge. Bound MC was washed through the filter under  $\text{N}_2$  by three successive 300- $\mu\text{l}$  washes with .1  $M$  Tris-HCl containing .1  $M$  NaCl. The pooled washings were counted in an LS 8100 scintillation counter (Beckman, Palo Alto, CA). Preliminary experiments at three concentrations MC (.25, 1.0, and 6.0 mM) determined that >97% of the added radioactivity could be accounted for in the combined first filtrate and three washings. Blank experiments without protein present were conducted at each concentration of MC. These blank values (which represent ~1% of total cpm or 5 to 8% of cpm bound to protein) were subtracted at each concentration.

#### Circular Dichroism Studies

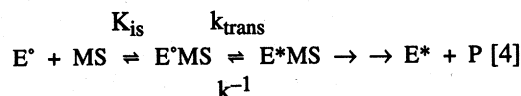
Protein samples for circular dichroism (CD) measurements were dialyzed for 12 to 16 h against buffer (.02  $M$  Tris-HCl, .04 to .08  $M$  KCl, pH 7.4) and filtered through Nucleopore (Pleasanton, CA) membrane filters (.4  $\mu\text{m}$ ) before use. Concentrated ligand solutions were added directly to the cuvettes from a microsyringe; total dilution of the enzyme did not exceed 4%. Circular dichroism spectra were recorded on a model J-41C spectropolarimeter (Jasco, LaJolla, CA) at ambient temperature ( $21 \pm 1^\circ\text{C}$ ) and analyzed as previously reported (28). Spectra presented in the figures are corrected for the solvent contributions (including all additives) and are expressed as molar ellipticity in the near UV and mean residue ellipticity in the far UV. Values of 112 for the mean residue molecular weight and .736 ml/g for the partial specific volume were calculated from the amino acid composition (28). The molecular weight of the dimeric form of mammary gland IDH (27) revised using a partial specific volume of .736 ml/g is 99,000

± 2000. Molar ellipticities were computed on the basis of a molecular weight of 49,500 for the subunit of IDH. The content of each type of secondary structure was estimated from the far UV CD spectrum (200 to 250 nm) with the aid of a computer program employing multiple linear regression analysis; reference spectra were either those of Chen et al. (5) or those of Stone et al. (30).

## RESULTS

### Stopped Flow Kinetics

In the determination of the Michaelis constant ( $K_m$ ) for DL-isocitrate for soluble NADP<sup>+</sup>:IDH (9), particularly at low metal ion concentrations, early nonlinear portions of the initial velocity curves were observed when the reaction was initiated with substrate. Examination of the early phases of the reaction progress curves in the stopped flow spectrophotometer showed a nonlinear response with a characteristic lag time prior to the achievement of a linear steady state (Figure 1a). This behavior was nearly abolished when the enzyme was preincubated with metal ion and substrate prior to mixing in the stopped flow apparatus (Figure 1b). Preincubation with NADP<sup>+</sup>, metal ion alone, or substrate alone did not appear to abolish the lag time, and results were nearly identical to those shown in Figure 1a. These preliminary results were consistent with an apparent MS-induced elimination of the lag time. Indeed, previous results on the soluble (9) and the mitochondrial forms (7) of NADP<sup>+</sup>:IDH have shown that MS is the true substrate for these enzymes. According to the theory for hysteretic enzymes (enzymes with nonlinear kinetics) as developed by Frieden (15), the enzyme can be considered to occur in two states, an initial (E<sup>o</sup>) and a final (E<sup>\*</sup>) state; substrate binding may then facilitate the transition between these states. Stopped flow experiments on NADP<sup>+</sup>:IDH were conducted without preincubation and at MS concentrations ranging from .1 to 10 times  $K_m$ . Each curve was analyzed by nonlinear regression techniques and fitted to various models (10). The best fit was obtained with a model in which the bound substrate causes the conversion of E<sup>o</sup>MS, which is inactive, to E<sup>\*</sup>MS, which is fully active. For this model, the general scheme given by Frieden (15) can be simplified to



where

- E<sup>o</sup> = inactive enzyme,
- E<sup>\*</sup> = active enzyme,
- $K_{is}$  = the dissociation constant for E<sup>o</sup>MS,
- $k_{trans}$  = the rate constant for the conversion of E<sup>o</sup>MS to E<sup>\*</sup>MS, and
- $k^{-1}$  = the reverse rate constant for E<sup>\*</sup>MS to E<sup>o</sup>MS.

The integrated form of the equation for appearance of product P was derived (10) and is

$$P_{obs} = V_F t - V_F \left( \frac{1 - e^{-kt}}{k} \right) \quad [5]$$

where

- $P_{obs}$  = concentration of observed product,
- $V_F$  = velocity of NADPH formation by the enzyme in state E<sup>\*</sup>,
- $k$  = rate constant for conversion of E<sup>o</sup>MS to E<sup>\*</sup>MS ( $k_{trans}$  of Equation [4]), and
- $t$  = time.

When the stopped flow data were fitted with Equation [5], excellent root mean squares were obtained, and the confidence levels for the fits were all in excess of 95%. Figure 1c shows an example of the actual fit of data to Equation [5]. This analysis also uses all data points obtained, as contrasted with graphical estimates (8), which require an arbitrary choice for the line drawn, and which ignore the actual data obtained earlier; an example of graphical analysis is when  $\tau$ , the lag time, and its reciprocal, the transition rate, are computed as shown in Figure 1a.

Given the applicability of Equation [5] (10), the effects of various preincubation conditions can now be placed on a more quantitative basis by solving for the transition rate, which in each experiment is the observed value. The results are given in Table 1. Preincubation with MS at 150  $\mu M$  produces a 10-fold increase in the observed value (relative to the enzyme alone), resulting in a lag time of only .56 s. Thus, even with preincubation, some lag time is observed; neither NADP<sup>+</sup> alone nor substrate

alone causes as large a decrease in lag time. Metal ion alone decreases the lag time, but not nearly to the same extent as MS.

#### Effects of MC on Activation

The stopped flow kinetics of NADP<sup>+</sup>:IDH was next studied to determine the effects of metal, citrate, and MC complex on the conversion rate constant (Equation [4]). When preincubated with MC alone at 1 mM, the lag time was drastically decreased (Table 2). At 5 mM, MC was as effective as MS at 150 μM in decreasing the lag time. Citrate alone can partially depress lag time, but not nearly as effectively as the MC complex. The stopped flow data indicate that the MC complex has the ability to activate the enzyme.

#### Far UV CD of IDH

The CD spectrum (200 to 250 nm) of IDH was studied (28). The curves closely fit the experimental data and were generated by assuming the following content of secondary structure: 41% α-helix, 32% β-form, and 13% β-turn. The theoretical curve generated using the method of Stone et al. (30) fits the experimental data more closely than those of Chen et al. (5). The presence of a saturating concentration of the MS complex failed to bring about any detectable change in the spectrum. Apparently, binding of the substrate does not alter the secondary structure of the enzyme. The far UV spectrum of mammary

gland IDH resembles that of the cytosolic isozyme from beef liver (3) and the mitochondrial form from pig heart (20). Mas and Colman (20) also failed to observe any influence of an analog of NADP or a mixture of substrate and coenzyme analog on the secondary structure of pig heart (mitochondrial) IDH.

#### Near UV CD of IDH

The near UV CD spectrum of IDH (Figure 2a) exhibits three main features: a positive band at ca. 292 nm, a negative band at ca. 278 nm, and a broad positive band centered at ca. 260 nm.

For the near UV CD spectrum of IDH, tentative band assignments were made on the basis of the known CD bands of tryptophan and tyrosine derivatives (29, 31, 32). Binding of MS by the enzyme dramatically alters the near UV CD spectrum of IDH (Figure 2a). The negative band at 278 nm attributed to tyrosine is greatly decreased in the presence of the substrate, but there is relatively no change in the positive band at 292 nm that is due to tryptophan. The spectral transition at 278 nm reaches completion at 41 μM MS; no further increase in molar ellipticity is observed when the concentration of MS is increased to 123 or 500 μM. The position and intensity of the band at 292 nm are also relatively unchanged. The CD spectrum of the enzyme was not modified by the addition of 600 μM isocitrate alone. Assuming that the enzyme is 90% saturated with the substrate at a concentration of 41 μM,

TABLE 1. Effects of various preincubation conditions on the observed rate constant ( $k_{obs}$ ) and the lag time ( $\tau$ ).<sup>1</sup>

Enzyme cosolutes <sup>2</sup>	$k_{obs}$ <sup>3</sup>		$\tau$ (s)	$V_F$ <sup>3</sup> (μmol/min per mg)
	Average	SEE		
Alone	.169	.015	5.92	30.4
With NADP <sup>+</sup>	.180	.013	5.55	29.5
With MS	1.76	.06	.56	38.3
With M <sup>2+</sup> <sub>T</sub>	.262	.014	3.82	32.2
With S <sub>T</sub>	.156	.017	6.38	37.4

<sup>1</sup>Average of three determinations using computer fitted data;  $\tau$  is defined as  $1/k_{obs}$ .

<sup>2</sup>Standard reaction concentrations, except the concentration of metal-substrate (MS) complex after mixing, was fixed at 150 μM, and the free Mn<sup>2+</sup> concentration was fixed at 80 μM. The total metal (M<sup>2+</sup><sub>T</sub>) was .245 mM, and the total substrate (S<sub>T</sub>) was 1.78 mM.

<sup>3</sup>The rate of conversion of inactive enzyme MS to active enzyme MS; SEE = standard error of estimate;  $V_F$  is the final velocity for NADPH formation.

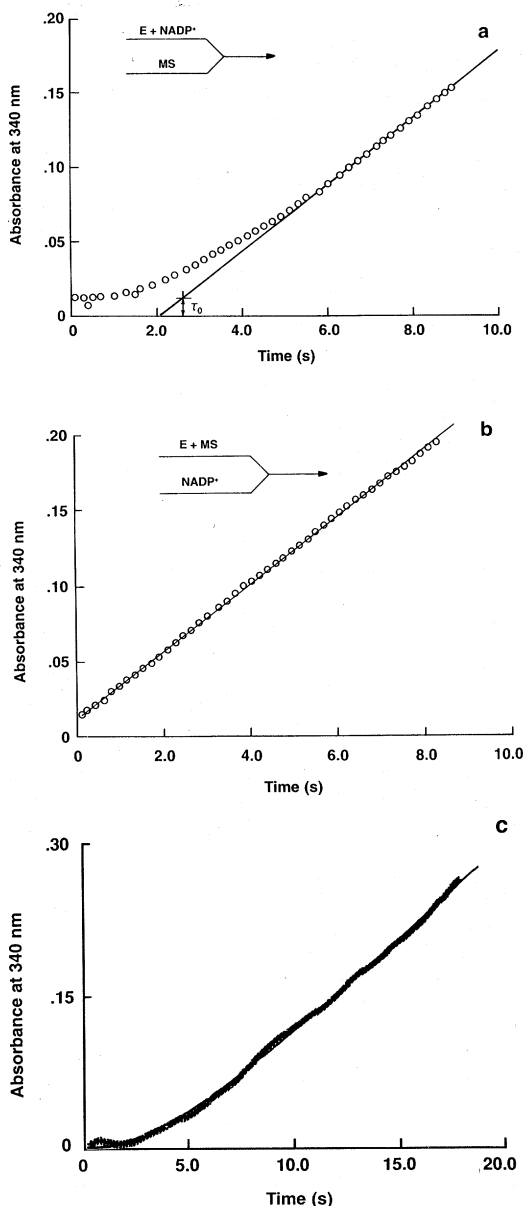


Figure 1. Time course of the reaction of  $\text{NADP}^+$  isocitrate dehydrogenase. The enzyme was incubated under two conditions in the syringes of the stopped flow spectrophotometer. The insets show the contents of the syringes prior to mixing. a) Enzyme (E) incubated with  $\text{NADP}^+$  only and b) enzyme incubated with metal-isocitrate complex (MS). Both syringes contain buffer, and the concentrations after mixing are the standard conditions of the assay. Each circle represents five data points. The final linear portion can be thought of as the final velocity; the intercept of this line at absorbance at 340 nm = 0 is the lag time,  $\tau$ ; its reciprocal is  $k$ . c) Actual computer fit of data, E not preincubated with MS.

the dissociation constant ( $K_d$ ) for the interaction of IDH with MS is estimated to be  $2.6 \mu\text{M}$ , which compares favorably with  $3.0 \mu\text{M}$  for  $K_m$  as determined from kinetic measurements (9).

The difference CD spectrum (28) generated by the binding of MS to IDH (Figure 2b) is similar to those induced in other enzymes (14, 18), which are attributed mainly to altered contributions of tyrosyl side chains. In the presence of the manganous-citrate at  $1 \text{ mM}$ , the negative molar ellipticity at  $278 \text{ nm}$  is slightly decreased. In a separate experiment, increasing the concentration of the MC to  $5 \text{ mM}$  further reduced the negative band at  $278 \text{ nm}$ . The maximum difference CD spectrum, which was generated by the addition of the MC complex, was about one-half of that observed with MS. Thus, the MC complex mim-

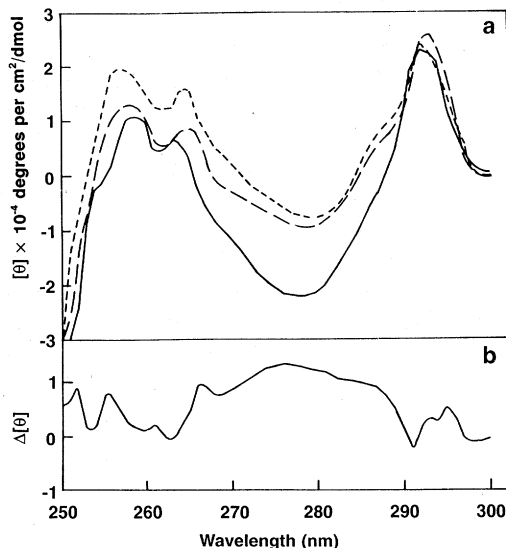


Figure 2. a) Near UV circular dichroism spectrum of isocitrate dehydrogenase (IDH) in the presence and absence of manganous-isocitrate. The enzyme concentration was  $12.4 \mu\text{M}$  in a buffer containing  $.02 \text{ M}$  Tris-HCl and  $.08 \text{ M}$  KCl at pH 7.4 with the following additions: none (—),  $170 \mu\text{M}$  threo- $\text{D}_3$  (+) isocitrate and  $510 \mu\text{M}$   $\text{MnSO}_4$  (---), and  $500 \mu\text{M}$  threo- $\text{D}_3$  (+) isocitrate and  $510 \mu\text{M}$   $\text{MnSO}_4$  (-----). The concentration of free  $\text{Mn}^{2+}$  was constant at  $280 \mu\text{M}$ , whereas the concentration of manganous-isocitrate varied from  $40 \mu\text{M}$  (---) to  $120 \mu\text{M}$  (-----). b) Difference circular dichroism spectrum. Difference curves were obtained by subtracting the spectrum of a mixture of IDH and  $40 \mu\text{M}$   $\text{Mn}^{2+}$ -isocitrate from the spectrum of the enzyme alone.  $\Delta$  = change;  $[\Theta]$  = molar ellipticity.

TABLE 2. Effects of various preincubation conditions on the observed rate constant ( $k_{\text{obs}}$ ) and the lag time ( $\tau$ ).<sup>1</sup>

Enzyme cosolute	$k_{\text{obs}}^2$ (1/s)	$\tau$ (s)
Alone	.169	5.92
With + MS, <sup>3</sup> 150 $\mu\text{M}$	1.76	.56
With + MC, 1 mM	1.38	.72
With + MC, 5 mM	2.46	.41
With + C <sub>total</sub> , 1 mM	.368	2.72
With + C <sub>total</sub> , 5 mM	.318	3.15

<sup>1</sup>Average of three determinations using computer fitted data;  $\tau$  is defined as  $1/k_{\text{obs}}$ .

<sup>2</sup>The observed rate of conversion of inactive enzyme MS to active enzyme MS.

<sup>3</sup>MS = Metal-isocitrate complex; MC = metal-citrate; C = citrate.

ics the behavior of the substrate, but at higher concentrations. Both MC and MS can activate IDH by eliminating the lag time, but MC appears to have multiple effects.

#### Alteration of Enzyme Activity in the Steady State by Citrate

In the case of human heart NADP<sup>+</sup>:IDH, a mitochondrial form of the enzyme, citrate has been reported to be a simple competitive inhibitor of DL-isocitrate (26), which was also the case in the present study for the soluble NADP<sup>+</sup>:IDH as well in steady-state experiments; data for citrate inhibition at 6, 9, and 12 mM fit the classical case of competitive inhibition. Replots of the slopes of the double reciprocal plots yield an inhibitor constant of 250  $\mu\text{M}$  for citrate alone. However, citrate may compete with isocitrate for metal ions, because MS is the true substrate. In turn, MC could be the true inhibitor. To test this hypothesis further, experiments were conducted using  $V_{\text{max}}$  conditions; concentrations of metal-threo-D<sub>5</sub>-isocitrate and free metal ion were fixed at 250 and 80  $\mu\text{M}$ , respectively, and concentrations of MC were then varied to produce the Dixon plot shown in Figure 3a (inset). The reciprocal of the velocity ( $1/v$ ) is plotted against calculated MC (inhibitor) concentrations. These plots are usually linear; however, distinct non-linearity can be seen in the plot.

The traditional analysis of the Dixon plot (the reciprocal of the velocity vs. inhibitor) has the same disadvantage as double reciprocal analysis of velocity versus substrate; that is,

such plots suppress the sensitivity of the best data found at lowest inhibitor concentration. By the use of nonlinear regression analysis, data can be directly fitted without the need for mathematical transformations or weighting factors (10). The Gauss-Newton procedure also provides a statistical evaluation of the constants and of the fit that allows for comparison of various mathematical models (21). Figure 3a shows the direct variance of velocity with inhibitor (MC). Initial curvature upward is clearly seen, followed by gradual decline with

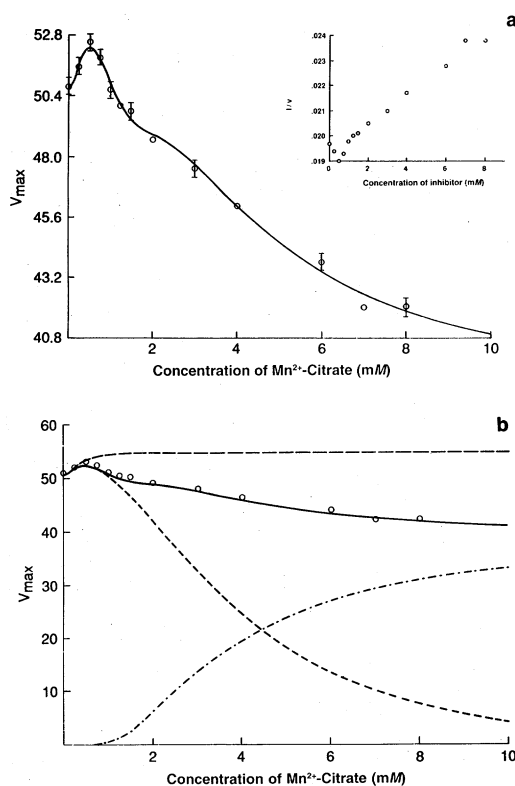


Figure 3. a) Inset: Dixon plot of  $1/\text{velocity}$  against the concentration of  $\text{Mn}^{2+}$ -citrate. Main plot of rate at conditions of maximum velocity (micromoles per minute per milligram) against the concentration of  $\text{Mn}^{2+}$ -citrate complex; the concentration of free  $\text{Mn}^{2+}$  was fixed at 80  $\mu\text{M}$  and that of  $\text{Mn}^{2+}$ -isocitrate at 250  $\mu\text{M}$ ; variations of  $\text{Mn}^{2+}$ -citrate were then calculated. Each point was run in triplicate; error bars represent the standard deviation. Data were computer fitted by nonlinear regression using the assumptions of thermodynamic linkage of velocity to binding of I ( $\text{Mn}^{2+}$ -citrate). b) Composite curve of Figure 3a (—) resolved into three component parts. Each component is in turn related to a term ( $V_i$ ) of the enzyme (—;  $V_1$ ), (---;  $V_2$ ), (- · - · -;  $V_3$ ).

a shoulder between 2 to 4 mM. Assuming that changes in the observed velocity (at constant: enzyme, cofactor, metal-substrate, and free metal concentrations) are thermodynamically linked to concentration-dependent binding of MC inhibitor concentrations, the data may then be analyzed by the linked function theory developed by Wyman (34) and utilized in our laboratory for study of metal ion-induced changes in protein solubilities (12). Statistical analysis (21) of the data with a variety of binding isotherms suggested the best curve to be composed of three distinct functions. This analysis, using Equation [3] as derived in Materials and Methods, is given in Table 3 for four experiments; it has the benefit of using the best data (low inhibitor, high velocity) for statistical fitting and provides a point of departure for discussion of the results. The analysis yields numbers for the association constant that in terms of  $K_d$ , can be related to physiological conditions (and possibly to enzyme structure through  $n$ ,  $m$ , and  $q$ ) and allows assessment of the individual relative contributions of predicted theoretical velocity to the observed total velocity.

#### Binding of MC

Studies on the binding of [ $^{14}\text{C}$ ]MC to IDH were carried out using porous membrane filters as described in Materials and Methods. Results of the binding studies are given in Figure 4,

and nonlinear regression analysis was used to fit the data with Equation [3]. Here  $v_i$  (moles of ligand bound per mole of monomer) replaces predicted theoretical velocity. The results of this analysis are consistent with the binding of up to 24 mol of MC/mol of IDH monomer. For the first transition observed,  $v_1$  was 4.3, and  $K_d = .257 \pm .049$  mM; the  $K_d$  is similar to that for MC activation ( $V_1$  in Table 3). The second transition of Figure 4 represents a class of sites with  $v = 10$  and  $K_d = 1.63 \pm .05$  mM; this  $K_d$  is close to the value found for  $V_3$  in Table 3. The third transition represents binding to an additional 10 sites with  $K_d = 3.02 \pm .04$  mM. These values probably are composites of a number of binding sites and actually represent average classes of sites (12, 34). The analysis of Figure 5 has an overall error of 3%.

#### Reevaluation of MS Data

The fact that MC complexes appear to have multiple effects on  $V_{\max}$  prompted a closer examination of the velocity of NADP<sup>+</sup>:IDH as a function of MS. Earlier studies (9) of the mammary enzyme had yielded a  $K_m$  of 3  $\mu\text{M}$  for the MS complex;  $V_{\max}$  was 52  $\mu\text{mol}/\text{min}$  per mg of protein. These studies were extended with additional points to .5 mM, and the observed inflection in  $V_{\max}$  was weak. When analyzed with Equation [3], the data (Figure 5a), yielded two values for  $K_m$  (3.1 and  $20.6 \pm 4.6$   $\mu\text{M}$ );  $V_{\max}$  were 46.6 and  $60.7 \pm 3.3$   $\mu\text{mol}/$

TABLE 3. Parameters obtained for linked function analysis of the variation of maximum velocity ( $V_{\max}$ ) with metal-citrate.<sup>1</sup>

State <sup>2</sup>	Exponents <sup>3</sup>	$k_i$	$K_d^4$		$V_i^5$	
			Average	SEE	Average	SEE
		(1/M)	(mM)		( $\mu\text{mol}/\text{min}$ per mg)	
$V_0$	...	...	...	...	50.7	.4
$V_1$	2	3790	.246	.113	54.6	2.1
$V_2$	2	260	3.83	.32	-3.0	6.3
$V_3$	4	650	1.54	.04	39.1	15.1

<sup>1</sup>Average values and error of coefficients for two complete and two partial runs each point in triplicate; total error of each individual fit averaged 1%.

<sup>2</sup>State of the enzyme  $\pm$  inhibitor (metal citrate):  $V_0$  = no inhibitor,  $V_1$  = first class of sites,  $V_2$  = second class of sites,  $V_3$  = third class of sites (c.f. Equation [1]).

<sup>3</sup>Integer exponents  $n$ ,  $m$ , and  $q$ .

<sup>4</sup>Calculated dissociation constant ( $1/k_i$ ), SEE = standard error of estimate.

<sup>5</sup> $V_i$  represents the predicted theoretical velocity contributed by each state and produced by the binding of each class of metal-citrate binding sites (cf. Equation [1]);  $V_0$  represents calculated maximum velocity in the absence of metal-citrate.

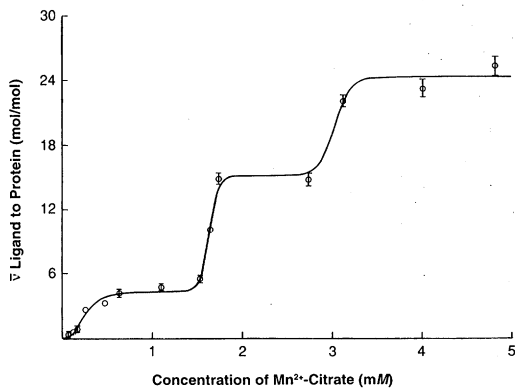


Figure 4. Binding of  $Mn^{2+}$ - $[^{14}C]$ citrate to  $NADP^+$ :isocitrate dehydrogenase (IDH); the number of moles of metal-citrate bound per mole of IDH are plotted against the concentration of free metal-citrate. The monomeric concentration of IDH was  $85.3 \mu M$ . The concentration of free  $Mn^{2+}$  was fixed at  $80 \mu M$ , and the concentration of metal-citrate varied. The experiment was conducted three times with two preparations of enzyme. Data points represent three to four replicates and error bars show standard deviations. The composite data were then computer fitted; the curve represents the best fit.

min per mg for the three experiments. Non-linear regression analysis was used to resolve this curve into its two component parts. This inflection would be difficult to analyze (Figure 5b) using conventional Lineweaver-Burk analysis. Attempting to split the data, which are apparently nonlinear, requires an arbitrary choice of points. When the data are analyzed directly, no changes in weighting factors are necessary, and the contributions of both functions are simultaneously evaluated. Addition of the second component enhanced the root mean square fit of the data significantly by three-fold(21). Thus, the data show that, at increased concentrations of MS, the enzyme activity is increased. Above  $25 \mu M$ , MS increases the rate so that  $V_{max}$  increases from a predicted 46.6 to  $60.7 \mu mol/min$  per mg, which is a greater stimulation by MS (~20%) than that of MC for which this effector produces a 10% increase over the enzyme in its absence (Table 3);  $K_d$  was  $21 \mu M$  for the second inflection point.

#### DISCUSSION

The apparent lack of  $NAD^+$ :IDH in bovine mammary gland (11) has led to the speculation that the activity of the soluble form of  $NADP^+$ :

IDH might be influenced by metabolites and, thus, in some way serve a regulatory function in this tissue and perhaps elsewhere. Work carried out primarily on heart (mitochondrial)  $NADP^+$ :IDH (3, 8) showed nonlinear kinetics under certain conditions, indicating a lag-burst hysteretic mechanism as delineated by Frieden (15). When the mammary  $NADP^+$ :IDH was injected into the stopped flow cell without prior incubation with MS, nonlinear progress curves were observed (Figure 1a). Such curves were first noted by Carlier and Pantaloni (3) for the cytosolic beef liver enzyme, but those authors made no calculations regarding the magnitude of the lag time, nor did they study its dependence on substrate concentration. In the current study, unique fits of these progress

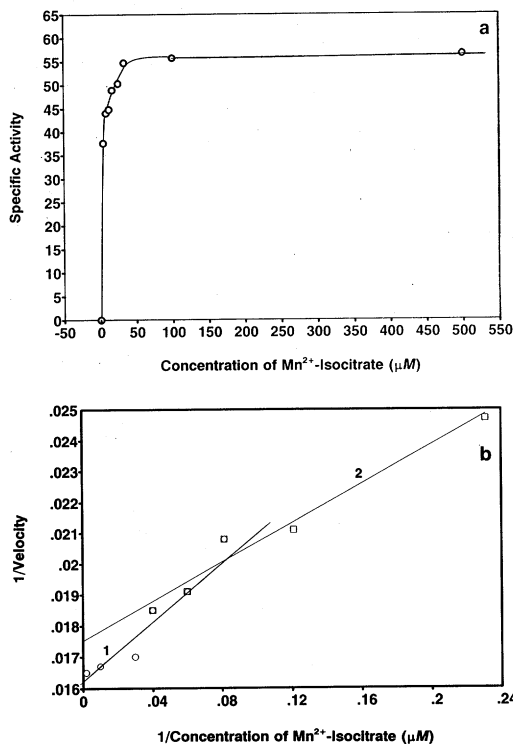


Figure 5. a) Variation of velocity in terms of specific activity (micromoles per minute per milligram) with metal-isocitrate as substrate. The concentration of free  $Mn^{2+}$  was fixed at  $100 \mu M$ , and the concentration of metal isocitrate varied; data points represent triplicate analysis. Data were computer fitted by nonlinear regression analysis. b) Traditional Lineweaver-Burk analysis of the same data; two possible lines (1 and 2) must be used to fit the data ( $\circ$  and  $\square$ ), respectively. An arbitrary choice in the cutoff is shown because some points ( $\circ$  and  $\square$ ) can be used for each line.

curves were obtained directly by nonlinear regression analysis with Equation [5]. This analysis allows for calculation of the observed rate constant for the transition from inactive to active form under a variety of conditions (e.g., Table 1). The rate constant values obtained herein by direct fitting are significantly lower than those given by Dalziel et al. (8) for heart (mitochondrial) enzyme; their values of .4/s were obtained graphically. The direct fitting of the reaction progress curve by Gauss-Newton nonlinear regression analysis as carried out herein allows for careful analysis of the data even when the lag is abolished visually and the observed rate is rather large (Table 1). This procedure was not followed in prior studies (3, 8).

The value of the rate constant for conversion of inactive to active enzyme (in analogy with  $V_{\max}$ ) can be thought of as the transition rate at saturation with MS and without preincubation (Equation [4]). The minimum transition time, the inverse of the conversion rate constant calculated for NADP<sup>+</sup>:IDH is 5 to 6 s and is relatively long considering that the rotational correlation time of a molecule such as IDH is of the order of  $10^{-9}$  s and that diffusion-controlled binding (the maximal upper rate) occurs at rates of the order of  $10^{11}$ /s. Thus, the rate-limiting step is probably not binding but perhaps is a slow conformational transition of the protein itself. Such transitions can range from a few milliseconds for an aromatic side chain rotation to minutes for large chain displacements (19). This transition is clearly catalyzed by MS (Table 1).

Also, MC can cause the same transition as MS from the inactive to the active form of NADP<sup>+</sup>:IDH, as calculated from Equation [4]. Preincubation with MC at 1 mM produces nearly a fourfold increase in the transition rate (Table 2). When the reciprocal of this constant (the minimum transition time, as discussed) is considered, 1 mM MC reduces the lag time to .72 s, which is nearly equivalent to preincubation with substrate (.56 s; Table 2). Preincubation with MC at 5 mM is as effective (.41 s) as MS in reducing the observed lag time (Table 2), but other changes also occur; MC reduces the velocity of NADPH reduction.

Changes observed in the near UV CD spectrum of IDH arise from an altered environment of tyrosine, tryptophan residues exposed to

solvent, or both in the enzyme-substrate complex. The involvement of tryptophan residues in these interactions cannot be excluded. However, the magnitude of the near UV difference CD, coupled with the failure to observe any changes in the acrylamide quenching of tryptophan fluorescence (28), suggests that the optical activity of other chromophores, primarily tyrosine, are influenced by the binding of MS. The altered environment of these chromophoric groups may signal a modification of the tertiary structure of the protein. Local interactions in the vicinity of a ligand-binding site may also be responsible for ellipticity changes in the absence of structural transitions (31, 32). For example, the electric field of a bound ion may induce a weak near UV CD band in an adjacent aromatic residue. The large changes accompanying the binding of ligands to IDH do not support the concept of a static mechanism. We suggest that the tertiary structure of IDH is modified by the binding of substrate or MC.

The data presented thus far do not rule out monomer-dimer association as rate-limiting, which has been proposed (3) on the basis of qualitative observations. Carlier and Pantaloni (3) suggested that ligand-induced association was the rate-limiting step for activation of the beef liver enzyme. In contrast, Bailey and Colman (1) did not observe concentration-dependent changes in enzyme activity for heart NADP<sup>+</sup>:IDH. In a recent study, Seery and Farrell (27) estimated  $K_d$  for dimer dissociation of mammary IDH to be 2 nM in the presence or absence of MS and MC. Under the conditions of the stopped flow experiments (60 nM), the enzyme thus exists essentially as a dimer. Those authors (27) also noted that decreases in activity occur for the enzyme when it is diluted and held in the absence of protectants, such as glycerol, MS complex, or serum albumin.

The total concentration of citrate in homogenized mammary gland is ~ 3 mM (13), but the calculated inhibitor constant (250  $\mu$ M), although in agreement with the literature for this metabolite, is much smaller; thus, MC should be the actual inhibitor. Analysis of velocity versus inhibitor (Figure 3a), using the assumptions of thermodynamic linkage, shows that MC binding has multiple effects; binding can indeed stimulate activity with a  $K_d$  of .25 mM; the maximum stimulation would be to

54.6  $\mu\text{mol}/\text{min}$  per mg or an 8% increase (Table 3). In contrast, binding to inhibitory sites with  $K_d = 3.83$  mM dramatically decreases activity with a predicted total repression of activity. At intermediate concentrations of MC, binding to sites with  $K_d = 1.54$  mM produces an apparent alleviation of inhibition (Table 3). This latter effect can be considered to be a reactivation. Thus, the curve of Figure 3a is the composite of these three interactions. Contributions from the various terms of Equation [3] are plotted individually in Figure 3b. The linked function analysis (Equation [3]) appears to provide a more quantitative basis for discussion of these phenomena than the Dixon plot. Because the best data (lowest inhibitor concentration) are used, the statistical fits are better, although qualitatively, the Dixon plot suggests a similar result. The average total citrate content of lactating bovine mammary gland is  $\sim 3$  mM, and the average free  $\text{Mg}^{2+}$  plus  $\text{Mn}^{2+}$  content  $>1$  mM (13); thus, these effects could occur in the physiological range.

In protein-ligand studies,  $n$ ,  $m$ , and  $q$  derived from Equation [3] have been correlated with the number of bound ligands giving rise to a selected change in properties (12), indicating, perhaps, that 2 mol of MC bind per dimer for activation to occur and that additional binding of 2 mol of MC complex leads to strong

inhibition, but binding of an additional 4 mol leads to modulation (Table 3). Interpreted another way, these exponents may be analogous to Hill coefficients (34) and could represent a measure of the degree of cooperativity within a class of sites. Direct binding studies of MC showed three classes of binding sites with a total of 24 mol of MC bound/mol of monomer. The first two classes have  $K_d$  comparable with those from linked function analysis of enzyme activity (.257 and 1.63, compared with .246 and 1.54 from Table 3). The third class has a  $K_d$  of 3.08, which is lower than 3.58 from Table 3. In each case, the number of actual binding sites ( $v$ ) was  $>n$ ,  $m$ , or  $q$  from Table 3. Although at first this finding appears to be contradictory, these values represent either relatively large numbers of individual sites with composite  $K_d$  or cooperativity within the classes of sites; e.g., the Hill coefficient is 3.0 for binding of 4 mol of  $\text{O}_2$  to hemoglobin (34). Furthermore, studies involving thermodynamic linkage contain the qualification that only binding sites causing a change in the measured parameter, in this case  $V_{\text{max}}$ , are disclosed by linkage; other binding not associated with changes in activity can occur (12). Similarly, inflections in the Michaelis curve can be treated quantitatively (Figure 5). Thus, linkage can be a more powerful means of uncovering

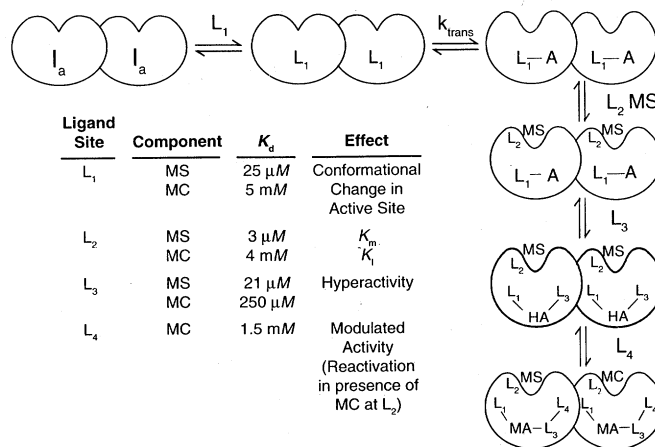


Figure 6. Summary of all possible states of NADP<sup>+</sup> isocitrate dehydrogenase (IDH) produced by the binding of metal-isocitrate (MS) and metal-citrate (MC). The enzyme as isolated is inactive ( $I_a$ ), binding of MS or MC removes the lag phase. This takes place at site  $L_1$ . Site  $L_2$  is the active site of the "activated" enzyme. Site  $L_3$  produces the hyperactivity (HA) observed for the enzyme in Figures 3 and 5. Site  $L_4$  corresponds to the reactivation for the MC-inhibited enzyme.

functional relationships than binding studies alone; changes in enzyme activity are used to follow only binding that influences activity.

Both MS and MC complexes can apparently play multiple roles in the modulation of NADP<sup>+</sup>:IDH. Figure 6 summarizes these effects with the assumption that all interactions with ligands occur with the dimer. Apparently, both MS and MC can "activate" the enzyme by alleviating the lag time. This activation is accompanied by a subtle conformational change (Figure 2). Whether this binding site (L<sub>1</sub>) is identical with the active site (L<sub>2</sub>) is not clearly established. Next, both MC and MS can bind to a second class of sites to stimulate the already activated enzyme, as demonstrated in the steady-state experiments (compare Figures 4 and 6). This hyperactivity site (L<sub>3</sub>) can be correlated with an independent binding site, at least in the case of MC (Table 3 and Figure 4); MS may bind to the same site, and its degree of stimulation is greater than that produced by MC. Finally, when MC has "apparently" served to inhibit IDH, binding of MC at L<sub>4</sub> can lead to reactivation giving modulated activity. The V<sub>max</sub> for this form is moderate at about 80% of maximum.

The analysis presented herein is in line with the random mechanism for NADP<sup>+</sup>:IDH proposed by Northrop and Cleland (24) based on steady state kinetics. The initial binding of metal-substrate or MC activates the enzyme, whether or not NADP<sup>+</sup> is present during the incubation.

### CONCLUSIONS

The importance of enzyme-substrate interactions in the regulation of enzymes has long been recognized (15), as have the principles of allosteric regulation (4, 16). The more recent focus on regulation through metal ion-activated cascades has emphasized the importance of regulatory binding sites with  $K_d \sim 10^{-9}$  (6). The data reported herein point to the potential significance of weaker binding sites as regulators of enzyme activity, because metabolite concentrations in mammary tissue occur in the same range as the derived constants. The effects of MC and MS observed in the stopped flow experiments on the enzyme are noteworthy, but only if the pools of Krebs cycle metabolites in mammary tissue oscillate

in the same fashion (1 to 5 s) as the glycolytic pools do in other tissues (23); under these circumstances, the 1- to 6-s lag times observed in this study could be relevant. From the linked function analysis, MC and MS can also cause hyperactivity, whereas higher MC concentrations produce either inhibition or modulation in the steady state. Thus, soluble NADP<sup>+</sup>:IDH could be positively and negatively controlled by the metabolite of the first step in the Krebs cycle, citrate synthesis, which occurs within the mitochondria (11, 17). Because Gabriel and Plaut (16) recently showed that MC may control NADP<sup>+</sup>:IDH as well, MC may play a more important role than previously expected in Krebs cycle metabolism in a variety of tissues.

### REFERENCES

- 1 Bailey, J. M., and R. F. Colman. 1985. Affinity labeling of NADP<sup>+</sup>-specific isocitrate dehydrogenase by a new fluorescent nucleotide analogue, 2-[(4-bromo-2,3-dioxobutyl) thio]-1, N<sup>6</sup>-ethenoadenosine 2',5'-bisphosphate. *Biochemistry* 24:5367.
- 2 Bauman, D. E., and C. L. Davis. 1974. Biosynthesis of milk fat. Page 31 in *Lactation*. B. L. Larson and V. R. Smith, ed. Vol. 2. Academic Press, New York, NY.
- 3 Carlier, M. F., and D. Pantaloni. 1973. NADP<sup>+</sup>-linked isocitrate dehydrogenase from beef liver. Purification, quaternary structure and catalytic activity. *Eur. J. Biochem.* 37:341.
- 4 Chen, R. F., and G.W.E. Plaut. 1963. Activation and inhibition of DPN-linked isocitrate dehydrogenase of heart by certain nucleotides. *Biochemistry* 2:1023.
- 5 Chen, Y., J. T. Yang, and K. H. Chau. 1974. Determination of the helix and  $\beta$  form of proteins in aqueous solution by circular dichroism. *Biochemistry* 13:3350.
- 6 Cheung, W. Y. 1984. Structure and function of calmodulin. *Fed. Proc.* 43:2995.
- 7 Colman, R. F. 1983. Aspects of the structure and functions of the isocitrate dehydrogenases. Page 41 in *Peptide and Protein Reviews*. M.T.W. Hearn, ed. Vol. 1. Marcel Dekker, Inc., New York, NY.
- 8 Dalziel, K., N. McFerran, B. Matthews, and C. H. Reynolds. 1978. Transient kinetics of NADP<sup>+</sup>-linked isocitrate dehydrogenase from bovine heart mitochondria. *Biochem. J.* 171:743.
- 9 Farrell, H. M., Jr. 1980. Purification and properties of NADP<sup>+</sup>: isocitrate dehydrogenase from lactating bovine mammary gland. *Arch. Biochem. Biophys.* 204: 551.
- 10 Farrell, H. M., Jr., J. T. Deeney, E. K. Hild, and T. F. Kumosinski. 1990. Stopped flow and steady state kinetic studies of the effects of metabolites on the soluble form NADP<sup>+</sup>:isocitrate dehydrogenase. *J. Biol. Chem.* 265:17637.
- 11 Farrell, H. M., Jr., J. T. Deeney, K. Tubbs, and R. A. Walsh. 1987. Role of isocitrate dehydrogenases and other Krebs cycle enzymes in lactating bovine mam-

- mary gland. *J. Dairy Sci.* 70:781.
- 12 Farrell, H. M., Jr., T. F. Kumosinski, P. Pulaski, and M. P. Thompson. 1988. Calcium-induced associations of the caseins: a thermodynamic linkage approach to precipitation and resolubilization. *Arch. Biochem. Biophys.* 265:146.
  - 13 Faulkner, A., and M. Peaker. 1982. Secretion of citrate into milk. *J. Dairy Res.* 49:159.
  - 14 Fretto, L., and E. H. Strickland. 1971. Use of circular dichroism to study the interactions of carboxypeptidase A (Anson) and  $A_{\alpha+\beta}$  with substrates and inhibitors. *Biochim. Biophys. Acta* 235:439.
  - 15 Frieden, C. 1979. Slow transitions and hysteretic behavior in enzymes. *Annu. Rev. Biochem.* 48:471.
  - 16 Gabriel, J. L., and G.W.E. Plaut. 1984. Citrate activation of NAD<sup>+</sup>-specific isocitrate dehydrogenase from bovine heart. *J. Biol. Chem.* 259:1622.
  - 17 Greville, G. D. 1969. Page 1 in *Citric Acid Cycle: Control and Compartmentation*. J. M. Lowenstein, ed. Marcel Dekker, Inc., New York, NY.
  - 18 Griffin, J. H., J. P. Rosenbusch, K. K. Weber, and E. R. Blout. 1972. Conformational changes in aspartate transcarbamylase. *J. Biol. Chem.* 247:6482.
  - 19 Karplus, M., and J. A. McCammon. 1983. Dynamics of proteins. *Annu. Rev. Biochem.* 52:263.
  - 20 Mas, M. T., and R. F. Colman. 1985. Spectroscopic studies of the interactions of coenzymes and coenzyme fragments with pig heart, oxidized NAD<sup>+</sup>-specific isocitrate dehydrogenase. *Biochemistry*. 24:1634.
  - 21 Meites, L. 1979. Some new techniques for analysis and interpretation of chemical data. *CRC Crit. Rev. Anal. Chem.* 8:1.
  - 22 Moore, J. H., and W. W. Christie. 1981. Lipid metabolism in the mammary gland. Page 227 in *Lipid Metabolism in Ruminant Animals*, W. W. Christie, ed. Pergamon Press, Elmsford, NY.
  - 23 Neet, K. E., and G. R. Ainslie, Jr. 1980. Hysteretic enzymes. *Methods Enzymol.* 64:192.
  - 24 Northrop, D. B., and W. W. Cleland. 1974. The kinetics of pig heart triphosphopyridine nucleotide-isocitrate dehydrogenase. *J. Biol. Chem.* 249:2928.
  - 25 Plaut, G.W.E., M. Cook, and T. Aogaichi. 1983. The subcellular location of isozymes of NADP<sup>+</sup>-isocitrate dehydrogenase in tissues of ox, pig, and rat. *Biochim. Biophys. Acta* 760:300.
  - 26 Seelig, G. F., and R. F. Colman. 1978. Characterization of the physicochemical and catalytic properties of human heart NADP-isocitrate dehydrogenase. *Arch. Biochem. Biophys.* 188:394.
  - 27 Seery, V. L., and H. M. Farrell, Jr. 1989. Physicochemical properties of isocitrate dehydrogenase from lactating bovine mammary gland. *Arch. Biochem. Biophys.* 274:453.
  - 28 Seery, V. L., and H. M. Farrell, Jr. 1990. Spectroscopic evidence for ligand-induced conformational change in NADP<sup>+</sup>-isocitrate dehydrogenase. *J. Biol. Chem.* 265:17644.
  - 29 Snow, J. W., and T. M. Hooker, Jr. 1975. Contribution of side-chain chromophores to the optical activity of proteins. *J. Am. Chem. Soc.* 97:3506.
  - 30 Stone, A. L., J. Y. Park, and R. E. Martenson. 1985. Low ultraviolet circular dichroism spectroscopy of oligopeptides 1-95 and 96-168 derived from myelin basic protein of rabbit. *Biochemistry* 24:6666.
  - 31 Strickland, E. H. 1974. Aromatic contributions to circular dichroism spectra of proteins. Page 113 in *Critical Reviews of Biochemistry*. E. D. Fasman, ed. Vol. 2. CRC Press, Cleveland, OH.
  - 32 Strickland, E. H., J. Horwitz, and C. Billups. 1969. Fine structure in the near-UV circular dichroism and absorption spectrum of tryptophan derivatives and chymotrypsinogen at 77°K. *Biochemistry* 8:3205.
  - 33 Szymanski, E. S., and H. M. Farrell, Jr. 1982. Isolation and solubilization of casein kinase from Golgi apparatus of bovine mammary gland and phosphorylation of peptides. *Biochim. Biophys. Acta* 702:163.
  - 34 Wyman, G., Jr. 1964. Linked functions and reciprocal effects in hemoglobin. *Adv. Protein. Chem.* 19:223.